



A multi-institutional study to evaluate the feasibility of next-generation sequencing and genomic analysis using formalin-fixed, paraffin-embedded biopsies of gastric cancer

Mitsuro Kanda¹ · Masanori Terashima² · Takahiro Kinoshita³ · Hiroshi Yabusaki⁴ · Masanori Tokunaga⁵ · Yasuhiro Kodera¹

Received: 23 September 2022 / Accepted: 3 November 2022 / Published online: 11 November 2022

© The Author(s) under exclusive licence to The International Gastric Cancer Association and The Japanese Gastric Cancer Association 2022

Abstract

Background Formalin-fixed, paraffin-embedded (FFPE) samples acquired and preserved adequately are expected to faithfully maintain tumor characteristics. Endoscopic biopsy tissues represent an attractive resource for identifying predictive biomarkers to evaluate pretreatment responses of patients with advanced gastric cancer (GC). However, whether genomic profiles obtained through next-generation sequencing (NGS) using biopsy samples match well with those gained from surgical FFPE samples remains a concern.

Methods We collected 50 FFPE samples (26 biopsies and 24 surgical samples) from patients with GC who participated in phase III clinical trial JCOG1509. The quality and quantity of FFPE samples were determined for deep sequencing using NGS. We queried a 435-gene panel CANCERPLEX-JP to generate comprehensive genomic profiling data including the tumor mutation burden (TMB).

Results The median DNA yields and NGS success rates of biopsy samples compared with surgical samples were 879 ng and 80.8% vs 8523 ng and 100%, respectively. Epstein-Barr virus and microsatellite instability-high were detected in 9.5% of biopsy samples. Comparing the genomic profiles of 18 paired samples for which NGS data were available, we detected identical somatic mutations in paired biopsy and surgical samples (kappa coefficient, 0.8692). TMB positively correlated between paired biopsy and surgical samples (correlation coefficient, 0.6911).

Conclusions NGS is applicable to the analysis of FFPE samples of GC acquired by the endoscopic biopsy, and the data were highly concordant with those obtained from surgical specimens of the same patients.

Keywords Gastric cancer · Next-generation sequencing · Formalin-fixed, paraffin-embedded sample · Endoscopic biopsy · Biomarker

Introduction

Despite the growing efficacy of postoperative adjuvant chemotherapy as a standard of care in Asia, locally advanced gastric cancer (GC) with lymph node metastases often recurs, requiring the development of more effective therapeutic strategies [1, 2]. Following the steps in the West, the addition of preoperative chemotherapy has been explored for highly selected patients, and more recently, for a wider range of patients with GC [3, 4]. However, surgery remains a mainstay of multidisciplinary treatment, and preoperative chemotherapy could merely prolong the time of surgery for the non-responders. In the era of personalized medicine, the establishment of methods to accurately predict the efficacy

✉ Mitsuro Kanda
m-kanda@med.nagoya-u.ac.jp

¹ Department of Gastroenterological Surgery, Nagoya University Graduate School of Medicine, 65 Tsurumai-Cho, Showa-Ku, Nagoya 466-8550, Japan

² Department of Gastric Surgery, Shizuoka Cancer Center, Shizuoka, Japan

³ Department of Gastric Surgery, National Cancer Center Hospital East, Kashiwa, Japan

⁴ Department of Gastroenterological Surgery, Niigata Cancer Center Hospital, Niigata, Japan

⁵ Department of Gastrointestinal Surgery, Tokyo Medical and Dental University, Tokyo, Japan

of preoperative chemo- or immunochemotherapy is eagerly awaited to select the optimal treatment strategy.

High-throughput next-generation sequencing (NGS), which comprehensively characterizes pathogenic genomic and transcriptional alteration, is among the most promising candidates for identifying biomarkers that predict treatment efficacy [5]. Samples used for such analyses are acquired either through biopsy or as surgically resected specimens. In the case of GC, biopsy samples are particularly attractive because they can be acquired easily and longitudinally using endoscopy [6]. These samples are generally preserved as formalin-fixed, paraffin-embedded (FFPE) tissue samples because of the simplicity of the process, storage and transportation [7, 8]. However, there are technical barriers to performing NGS using FFPE biopsy samples. For example, DNA extracted from FFPE tissues may be degraded, and intact DNA may be cross-linked through chemical modifications [8, 9]. Moreover, endoscopic samples may be too small for extraction of a sufficient amount of DNA and may suffer from the inherent issue of heterogeneity in GC in which the admixture of diverse histological phenotypes within a lesion is well documented [10]. Therefore, the feasibility of applying NGS to FFPE GC biopsy samples must be assessed. Moreover, GC is a highly genotypically heterogeneous disease with diverse histological phenotypes [1, 11]. Therefore, an important consideration is the acquisition of genomic information related to cancer characteristics that are identical between biopsy and surgical samples.

Here, we evaluated the feasibility of FFPE biopsy samples by comparing DNA sequences obtained by NGS using FFPE biopsy samples and surgical samples collected from the same patients who were enrolled in phase III JCOG1509 trial by the Stomach Cancer Study Group of the Japan Clinical Oncology Group (JCOG).

Patients and methods

Patient selection

FFPE samples (26 biopsy and 24 surgical) were collected from patients enrolled in the JCOG1509 trial (jRCTs031180350) who were treated at four of the participating institutions: the Shizuoka Cancer Center, National Cancer Center Hospital East, Niigata Cancer Center Hospital, or Nagoya University Hospital. The eligibility criteria of the JCOG1509 trial were as follows: (1) histologically proven gastric adenocarcinoma, (2) clinical T3-4/N+ by imaging, (3) no distant metastasis according to contrast-enhanced CT scans, (4) macroscopic tumor type neither Borrmann type 4 or large (≥ 8 cm) type 3, (5) no gastric stump cancer, (6) no prior chemotherapy, radiotherapy, or endocrine therapy for any malignancy within 5 years, (7)

age 20–79 years, (8) Eastern Cooperative Oncology Group performance status 0 or 1, and (9) sufficient organ and bone marrow function.

Sample preparation

Endoscopic biopsy samples acquired before treatment were immediately placed in 10% neutral-buffered formalin and fixed for 6–48 h at room temperature. The number of biopsy specimens was not prescribed in the protocol of JCOG1509 trial. Formalin-fixed tissues underwent serial processing and were then embedded in paraffin to create FFPE blocks. Sections 10- μ m thick were prepared from each FFPE block. Surgical specimens were immersed in 10% buffered formalin solution within 30 min of removal and were processed within 72 h after fixation. Sections 10- μ m thick were prepared by selecting areas ≥ 25 mm² containing $\geq 50\%$ GC components. The GC components of the samples stained with hematoxylin and eosin (HE) were encircled by cytopathologists. All FFPE samples were anonymized using the Biobank Japan-ID, and information that identified individual patients, including sex and age, was masked.

DNA extraction and quality control

DNA was extracted from unstained FFPE sections from biopsy ($n=26$) and surgical ($n=24$) samples. Using guide HE-stained slides, the cancer cell-enriched areas in the unstained tissue sections were scraped using the sharp edge of a sterilized razor blade. The tissue slices were collected into a 1.5 ml DNA LoBind tube (Eppendorf, Hamburg, Germany). DNA was extracted using a QIAamp DNA FFPE Tissue Kit (QIAGEN, Hilden, Germany). For quality control, extracted genomic DNA (gDNA) was evaluated by measuring DNA Integrity Number (DIN) using a TapeStation (Agilent Technologies, Santa Clara, CA, USA). The Quant-iT dsDNA Assay Kit (High Sensitivity) was used to determine DNA concentrations (Thermo Fisher Scientific).

NGS

Fragment libraries were prepared from 50 to 150 ng of DNA and enriched using the 435-gene panel of the clinically validated CANCERPLEX-JP (Denka Kew Genomics, Tokyo, Japan), which is enriched in coding regions and selected introns of genes with known associations with cancer [12]. Sequencing was performed using the Illumina MiSeq and NextSeq platforms (Illumina, San Diego, CA, USA) with an average 500 \times sequencing depth. Details of artifact and mutation data processing were previously described [7, 12]. For somatic mutations (single-nucleotide substitutions, indels, or both) a cutoff = 5% mutant allele frequency was used for the determination of artifact and 10% mutant allele frequency

was used for comparison between the paired biopsy and surgical samples. The tumor mutation burden (TMB), defined as the rate of amino acid codon-changing single-nucleotide variants (SNVs) per Mb, was determined for all samples [12]. To estimate the TMB, we retained SNVs with a mutation allelic fraction ≥ 0.1 after standard filtering and with high or moderate putative impact. Determination of microsatellite instability (MSI) was based on an extended loci panel. We analyzed the Bethesda panel as well as a collection of ≤ 950 regions comprising tandem repeats with minimum repeats of 1, 2, or 3 nucleotides in a stretch of 10 nucleotides [12, 13]. The number of indels within the region of interest was calculated, and tumors were classified as MSI-high or microsatellite stable (MSS). Tumors were analyzed for the presence of Epstein-Barr virus (EBV) sequences (reference genomes, NC_007605). The percentages of the total numbers of reads mapped to viral genomes were calculated, and samples were judged positive according to an empirical cutoff value = 0.0005% of reads mapped to EBV genomes [7, 12].

Statistical analysis

The significance of an association between two variables was assessed using Spearman's rank correlation coefficient [14]. Quantitative variables were compared using the Mann–Whitney U test. To statistically evaluate the percent agreement of mutations detected in paired biopsy and surgical samples, Cohen's Kappa was used. Statistical analyses were performed using JMP Pro version 16.1 (SAS Institute, Cary, NC). $P < 0.05$ indicates a significant difference.

Results

Sample conditions, gDNA yields, and availability of NGS data

Sample conditions, amounts of gDNA, DIN, and sequencing results of 26 biopsy and 24 surgical FFPE tissues are listed in Table 1. The median tissue volume of biopsy samples was 1.35 mm³ (range 0.36–5.80 mm³), and the median DNA yield was 879 ng (range 105–5131 ng). NGS data were available for 21 of 26 biopsy samples, indicating that the success rate of NGS was 80.8%. Compared with the samples in which NGS data were available, DNA yields of NGS failures were lower (median 1092 ng vs 119 ng; $P = 0.0076$), with lower DNA fragmentation rates (median 70.7% vs 29.1%; $P = 0.0018$). DIN values were significantly higher in NGS successes than in failures, (median 2.5 vs 2.1; $P = 0.040$). The 14 biopsy samples that met the minimum area of 7.4 mm² (i.e. 1.48 mm³) had successful NGS analyses. A positive correlation was observed

between the number of biopsies and tissue volume (correlation coefficient, 0.5197; $P = 0.0110$).

The median tissue volume of surgical samples was 8.0 mm³ (range 0.49–32.7 mm³), the median DNA yield was 8523 ng (range 159–41,300 ng), and the lowest DIN value was 2.3. NGS data were obtained from all 24 surgical samples.

Mutation status

All tumor samples had somatic mutations (single-nucleotide substitutions, indels, or both). The most frequently mutated gene among 21 biopsy samples was *TP53* (57.1%), followed by *FOXO1* (42.9%), *ZFHX3* (42.9%), and *ARID1B* (38.1%). We next compared the patterns of somatic mutations between biopsy and surgical samples. There were no mutations specifically detected in two or more biopsy samples. Figure 1a shows a mutation map of the 33 genes with mutations in ≥ 3 biopsy samples. Figure 1b displays the number of patients in which the mutation was commonly detected in biopsy and surgical samples as well as the number of patients in which the mutation was detected in one or the other. Kappa coefficient was calculated for 33 genes with mutations in ≥ 3 biopsy samples in 18 patients with paired FFPE samples and determined at 0.8692, representing high consistency in paired biopsy and surgical samples. These findings indicate that for most genes, the same mutations were detected in paired biopsy and surgical samples (Fig. 1).

Analysis of TMB, MSI, and EBV status

The results for TMB, MSI, and EBV status, which represent important genetic alterations in GC, other than mutations, are summarized in Table 2. The median TMB was 18.47 (range 10.01–29.25) for biopsy samples and 17.32 (range 11.55–23.86) for surgical samples. When we examined paired samples of the 18 patients for which NGS data were available for both samples, TMB values in biopsy samples positively correlated with those of surgical samples (correlation coefficient, 0.6911; $P = 0.0015$) (Fig. 2). However, concordance was not sufficient in other items. MSI-high was detected in 2 of 21 biopsy samples (9.5%). Of these two patients, paired surgical samples were unavailable in one, whereas the surgical specimen of the remaining patient was found to be MSS. Likewise, whereas EBV status was positive in 2 of 21 (9.5%) of the biopsy samples, one of these was EBV-negative in the paired surgical samples.

Discussion

Precision medicine utilizing NGS is expected to bring a paradigm shift from a pathological microscopic-based approach to a genetic signature-based diagnosis [13, 15]. This concept

Table 1 Sample conditions and sequencing results of 50 formalin-fixed and paraffin-embedded tissue samples

Case	Biopsy	Surgical specimen												
		Area (mm ²)	Volume (mm ³)	Number of pieces	Amount of DNA (ng)	DIN	Fragmentation rate (%)	NGS	Area (mm ²)	Volume (mm ³)	Amount of DNA (ng)	DIN	Fragmentation rate (%)	NGS
1		14.1	2.82	4	2356	4.0	88.6	Success	84.2	8.42	3423	5.6	85.2	Success
2		16.6	3.32	3	770	2.5	50.1	Success	263.2	26.32	25,970	3.1	81.1	Success
3		15.2	3.04	7	1092	2.6	31.9	Success	326.6	32.66	24,780	2.4	65.5	Success
4		6.1	1.22	2	116	2.1	23.1	Failure	45.3	4.53	3626	2.6	81.5	Success
5		4.0	0.80	2	263	1.9	43.7	Failure	55.3	5.53	7350	2.3	79.6	Success
6		1.8	0.36	1	252	2.5	59.2	Success	241.9	24.19	16,835	2.7	78.8	Success
7		3.6	0.72	3	574	2.3	30.7	Success	11.3	1.13	1159	2.6	75.7	Success
8		17.5	3.50	3	826	2.2	73.4	Success	123.2	12.32	9695	2.8	73.4	Success
9		1.9	0.38	2	105	1.8	32.4	Failure	213.6	21.36	23,363	3.0	84.1	Success
10		8.2	1.64	2	2471	2.2	83.0	Success	12.8	1.28	2839	3.7	87.4	Success
11		20.8	4.16	5	5131	3.9	85.3	Success	198.5	19.85	11,970	3.6	86.0	Success
12		10.8	2.16	3	2271	3.1	88.0	Success	4.9	0.49	1264	3.5	88.3	Success
13		4.4	0.88	3	1848	2.8	66.0	Success	109.8	10.98	11,550	3.7	74.4	Success
14		7.4	1.48	2	830	2.8	82.7	Success	291.3	29.13	41,300	3.8	83.0	Success
15		9.0	1.80	3	875	2.0	74.6	Success	76.3	7.63	6342	4.3	84.6	Success
16		3.0	0.60	2	424	1.6	59.5	Success	44.9	4.49	5663	3.3	87.8	Success
17		3.8	0.76	2	718	2.8	74.9	Success	105.0	10.50	18,137	3.0	42.8	Success
18		6.0	1.20	2	641	2.1	56.4	Success	13.4	1.34	3500	4.1	73.3	Success
19		30.5	5.80	7	2520	2.5	58.0	Success	15.7	1.57	3269	3.0	76.9	Success
20		13.0	2.60	3	1950	2.4	49.4	Success						
21		14.8	2.96	5	2272	2.2	79.3	Success						
22		11.2	2.24	2	1547	1.7	70.7	Success						
23		4.3	0.86	5	882	3.4	71.7	Success	58.5	5.85	7168	3.8	74.2	Success
24		1.8	0.36	4	119	2.2	4.1	Failure	12.3	1.23	1890	4.5	80.3	Success
25		4.8	0.96	6	889	2.3	29.1	Failure	103.4	10.34	21,798	3.7	74.4	Success
26									61.8	6.18	14,588	3.8	80.4	Success
27		10.4	2.08	9	2723	2.9	62.8	Success	150.6	15.06	20,286	3.4	72.6	Success

DIN/DNA integrity number, NGS next-generation sequencing

Table 2 Tumor mutation burden, microsatellite instability and Epstein-Barr virus status of 50 formalin-fixed and paraffin-embedded tissue samples

Case	Biopsy			Surgical specimen		
	Tumor mutation burden	Microsatellite instability	Epstein-Barr virus	Tumor mutation burden	Microsatellite instability	Epstein-Barr virus
1	16.17	MSS	Negative	18.47	MSS	Negative
2	21.55	MSS	Negative	23.86	MSS	Negative
3	16.17	MSS	Positive	13.09	MSS	Negative
4				13.86	MSS	Negative
5				22.32	MSS	Negative
6	13.86	MSS	Negative	16.93	MSS	Negative
7	18.47	MSS	Negative	16.17	MSS	Negative
8	25.40	MSS	Negative	22.32	MSS	Negative
9				19.24	MSS	Negative
10	13.86	MSS	Negative	15.40	MSS	Negative
11	19.24	MSS	Negative	17.70	MSS	Negative
12	19.24	MSS	Negative	16.93	MSS	Negative
13	14.63	MSS	Negative	17.70	MSS	Negative
14	16.93	MSS	Negative	18.47	MSS	Negative
15	21.55	MSS	Positive	16.17	MSS	Positive
16	28.48	MSI-H	Negative	22.32	MSS	Negative
17	22.32	MSS	Negative	21.55	MSS	Negative
18	10.01	MSS	Negative	13.86	MSS	Negative
19	20.78	MSS	Negative	23.09	MSS	Negative
20	23.86	MSS	Negative			
21	29.25	MSS	Negative			
22	14.63	MSI-H	Negative			
23	18.47	MSS	Negative	20.01	MSS	Negative
24				11.55	MSS	Negative
25				14.63	MSS	Negative
26				14.63	MSS	Negative
27	14.63	MSS	Negative	13.09	MSS	Negative

MSS microsatellite stable, MSI-H microsatellite instability high

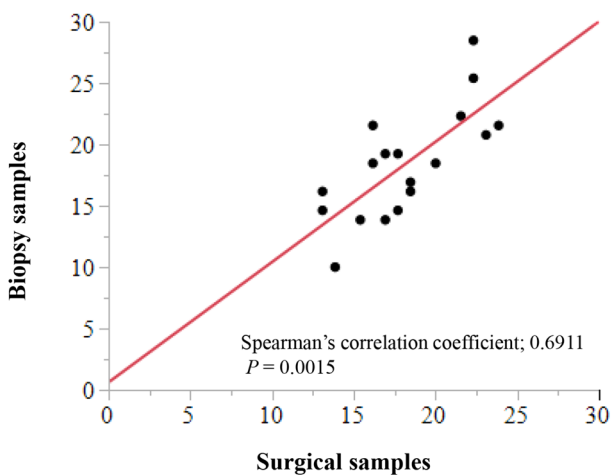


Fig. 2 Tumor mutation burden of biopsy and surgical specimens

chemotherapy [24, 25]. Taken together, our data indicate that FFPE biopsy samples will serve as an adequate source of genomic information for GC tissues.

MSI, EBV status, and TMB are sources of important genomic information that correlates with the response to chemotherapy or immune-checkpoint inhibitors [26]. The frequencies of MSI-high are 6.6–9.7% in cases of resectable GC in Asia [27, 28]. Furthermore, 6.7% of Japanese patients with unresectable GC who underwent MSI testing are MSI-high [29]. EBV-associated GC accounts for 7–10% of these patients [30]. Our present analysis of biopsy FFPE samples reveals that MSI-high and EBV were detected as frequently as reported by others. Pathological complete response by preoperative chemotherapy was observed in one case of MSI-high at biopsy so that the corresponding surgical sample was unavailable. The CANCERPLEX-JP protocol defines a cutoff value of 26 or more indels for determining MSI-high [12]. In the other case, the biopsy sample

was determined to be MSI-High with an indel value of 26, while the surgical specimen was determined to be MSS with a value of 22, slightly below the cutoff. Diagnostic accuracy near the cutoff value remains to be a technical challenge. EBV status was negative in the surgical sample in one of the two cases that had positive EBV in biopsy samples. We speculate that this discrepancy attributed to intratumor heterogeneity. The heterogeneity of gastric cancer should be considered. However, because the main purpose of this study was to determine whether genomic profiles can be obtained from FFPE biopsy samples, biopsy tissues were combined to achieve maximum yield of gDNA. To assess how much the genomic information changes in different sites of biopsy from the primary tumor of the same patient will be desirable in future studies. On the other hand, we show here that TMB of 18 paired samples positively correlated between the values of biopsy and surgical samples. These findings are consistent with those of somatic mutation analysis; and the data support the concordance of genomic data between biopsy and surgical FFPE samples.

Our present results will likely contribute to the design of biomarker studies of GC. Biomarkers are required to predict the efficacy of preoperative chemotherapy when applied to tissue specimens collected before the administration of therapy. The concerns that are raised when NGS is used only to analyze surgically resected samples are as follows: (1) Cancer tissue cannot be obtained when a complete pathological response is achieved before preoperative chemotherapy. (2) A large amount of necrotic tissue due to the preoperative chemotherapy could contaminate the tumors. (3) Only genomic abnormalities in the sampled area are evaluated because of the heterogeneity of GC. (4) Specimen will become unavailable when surgery is contraindicated because of progressive disease during preoperative chemotherapy [6, 25, 31]. In the present study, the concordance of genomic data between biopsy and surgical samples was high, including patients who received preoperative treatment. If the DNA yield is sufficient to perform NGS, we conclude that pretreatment biopsy FFPE samples represent an ideal source of genomic data to identify biomarkers that predict the efficacy of preoperative chemotherapy. Moreover, FFPE samples can be stored virtually indefinitely and are available from all GC patients who undergo endoscopy. The protocol of this feasibility study stipulated that only FFPE specimens were to be collected, and patient consent was obtained based on this protocol. Therefore, validation experiments using frozen tissues are impracticable this time. Collection of frozen tissues has been initiated for a future biomarker study accompanying the JCOG1509 trial, where the consistency of the genomic data between frozen and FFPE samples will be evaluated.

The present study has several limitations. First, we analyzed a limited number of samples. Furthermore, the samples

were derived from patients participating in an ongoing phase III clinical trial JCOG1509, and, therefore, data pertaining to clinical information, including treatment groups (preoperative chemotherapy group or not), are masked. Therefore, the correlation analysis between genomic data and clinical factors will not be disclosed until the completion of JCOG1509.

Conclusion

In summary, we demonstrate here that NGS can be performed using FFPE samples prepared from endoscopic biopsies as well as from surgically resected GC tissues. Genomic data obtained from pretreatment endoscopic biopsy samples showed high concordance with data for surgical samples from the same patients.

Acknowledgements We are grateful to DENKA Corporation for your kind cooperation on the cancer panel analysis (CANCERPLEX-JP). We thank Edanz (<https://jp.edanz.com/ac>) for editing a draft of this manuscript.

Declarations

Conflict of interest A potential conflict of interest exists because DENKA Corporation performed the cancer panel analysis (CANCERPLEX-JP) free of charge. However, only anonymized identification numbers for all samples were disclosed, and all medical information including age and gender were masked. This prevented the results of the cancer panel analysis from being represented as favorable to DENKA Corporation, which had no influence on the planning, implementation, and results of the study.

Ethical approval All procedures were in accordance with the ethical standards of the responsible committees on human experimentation (institutional and national) and with the Helsinki Declaration of 1964 and later versions.

Informed consent Written informed consent for the JCOG1509 trial and the present study was obtained from all patients as required by the Institutional Review Board of each participating institution.

References

1. Smyth EC, Nilsson M, Grabsch HI, van Grieken NC, Lordick F. Gastric cancer. *Lancet*. 2020;396:635–48.
2. Kanda M, Shimizu D, Sawaki K, Nakamura S, Umeda S, Miwa T, et al. Therapeutic monoclonal antibody targeting of neuronal pentraxin receptor to control metastasis in gastric cancer. *Mol Cancer*. 2020;19:131.
3. Kang YK, Yook JH, Park YK, Lee JS, Kim YW, Kim JY, et al. PRODIGY: a phase III study of neoadjuvant docetaxel, oxaliplatin, and S-1 plus surgery and adjuvant S-1 versus surgery and adjuvant S-1 for resectable advanced gastric cancer. *J Clin Oncol*. 2021;39:2903–13.
4. Zhang X, Liang H, Li Z, Xue Y, Wang Y, Zhou Z, et al. Perioperative or postoperative adjuvant oxaliplatin with S-1 versus adjuvant oxaliplatin with capecitabine in patients with locally advanced gastric or gastro-oesophageal junction adenocarcinoma

- undergoing D2 gastrectomy (RESOLVE): an open-label, superiority and non-inferiority, phase 3 randomised controlled trial. *Lancet Oncol.* 2021;22:1081–92.
5. Katona BW, Rustgi AK. Gastric cancer genomics: advances and future directions. *Cell Mol Gastroenterol Hepatol.* 2017;3:211–7.
 6. Kleo K, Jovanovic VM, Arndold A, Lehmann A, Lammert H, Berg E, et al. Response prediction in patients with gastric and esophagogastric adenocarcinoma under neoadjuvant chemotherapy using targeted gene expression analysis and next-generation sequencing in pre-therapeutic biopsies. *J Cancer Res Clin Oncol.* 2022. <https://doi.org/10.1007/s00432-022-03944-z>.
 7. Nagahashi M, Shimada Y, Ichikawa H, Nakagawa S, Sato N, Kaneko K, et al. Formalin-fixed paraffin-embedded sample conditions for deep next generation sequencing. *J Surg Res.* 2017;220:125–32.
 8. McDonough SJ, Bhagwate A, Sun Z, Wang C, Zschunke M, Gorman JA, et al. Use of FFPE-derived DNA in next generation sequencing: DNA extraction methods. *PLoS ONE.* 2019;14:e0211400.
 9. Einaga N, Yoshida A, Noda H, Suemitsu M, Nakayama Y, Sakurada A, et al. Assessment of the quality of DNA from various formalin-fixed paraffin-embedded (FFPE) tissues and the use of this DNA for next-generation sequencing (NGS) with no artifactual mutation. *PLoS ONE.* 2017;12:e0176280.
 10. Hulten KG, Genta RM, Kalfus IN, Zhou Y, Zhang H, Graham DY. Comparison of culture with antibiogram to next-generation sequencing using bacterial isolates and formalin-fixed paraffin-embedded gastric biopsies. *Gastroenterology.* 2021;161:1433–42.e2.
 11. Network CGAR. Comprehensive molecular characterization of gastric adenocarcinoma. *Nature.* 2014;513:202–9.
 12. Eifert C, Pantazi A, Sun R, Xu J, Cingolani P, Heyer J, et al. Clinical application of a cancer genomic profiling assay to guide precision medicine decisions. *Per Med.* 2017;14:309–25.
 13. Ichikawa H, Nagahashi M, Shimada Y, Hanyu T, Ishikawa T, Kameyama H, et al. Actionable gene-based classification toward precision medicine in gastric cancer. *Genome Med.* 2017;9:93.
 14. Kanda M, Suh YS, Park DJ, Tanaka C, Ahn SH, Kong SH, et al. Serum levels of ANOS1 serve as a diagnostic biomarker of gastric cancer: a prospective multicenter observational study. *Gastric Cancer.* 2020;23:203–11.
 15. Jeon J, Cheong JH. Clinical implementation of precision medicine in gastric cancer. *J Gastric Cancer.* 2019;19:235–53.
 16. Hirano H, Abe Y, Nojima Y, Aoki M, Shoji H, Isoyama J, et al. Temporal dynamics from phosphoproteomics using endoscopic biopsy specimens provides new therapeutic targets in stage IV gastric cancer. *Sci Rep.* 2022;12:4419.
 17. Sato Y, Okamoto K, Kawaguchi T, Nakamura F, Miyamoto H, Takayama T. Treatment response predictors of neoadjuvant therapy for locally advanced gastric cancer: current status and future perspectives. *Biomedicines.* 2022;10:1614.
 18. McLean MH, El-Omar EM. Genetics of gastric cancer. *Nat Rev Gastroenterol Hepatol.* 2014;11:664–74.
 19. Duraes C, Almeida GM, Seruca R, Oliveira C, Carneiro F. Biomarkers for gastric cancer: prognostic, predictive or targets of therapy? *Virchows Arch.* 2014;464:367–78.
 20. Razzak M. Genetics: new molecular classification of gastric adenocarcinoma proposed by The Cancer Genome Atlas. *Nat Rev Clin Oncol.* 2014;11:499.
 21. Yuan L, Xu ZY, Ruan SM, Mo S, Qin JJ, Cheng XD. Long non-coding RNAs towards precision medicine in gastric cancer: early diagnosis, treatment, and drug resistance. *Mol Cancer.* 2020;19:96.
 22. Niu D, Li L, Yu Y, Zang W, Li Z, Zhou L, et al. Evaluation of next generation sequencing for detecting HER2 copy number in breast and gastric cancers. *Pathol Oncol Res.* 2020;26:2577–85.
 23. Sakaguchi T, Nishii Y, Iketani A, Esumi S, Esumi M, Furuhashi K, et al. Comparison of the analytical performance of the Oncomine dx target test focusing on bronchoscopic biopsy forceps size in non-small cell lung cancer. *Thorac Cancer.* 2022;13:1449–56.
 24. Kwon M, An M, Klempner SJ, Lee H, Kim KM, Sa JK, et al. Determinants of response and intrinsic resistance to PD-1 blockade in microsatellite instability-high gastric cancer. *Cancer Discov.* 2021;11:2168–85.
 25. Nakamura Y, Kawazoe A, Lordick F, Janjigian YY, Shitara K. Biomarker-targeted therapies for advanced-stage gastric and gastro-oesophageal junction cancers: an emerging paradigm. *Nat Rev Clin Oncol.* 2021;18:473–87.
 26. Lee KW, Van Cutsem E, Bang YJ, Fuchs CS, Kudaba I, Garrido M, et al. Association of tumor mutational burden with efficacy of pembrolizumab±chemotherapy as first-line therapy for gastric cancer in the phase III KEYNOTE-062 study. *Clin Cancer Res.* 2022;28:3489–98.
 27. Smyth EC, Wotherspoon A, Peckitt C, Gonzalez D, Hulkki-Wilson S, Eltahir Z, et al. Mismatch repair deficiency, microsatellite instability, and survival: an exploratory analysis of the medical research council adjuvant gastric infusional chemotherapy (MAGIC) trial. *JAMA Oncol.* 2017;3:1197–203.
 28. Choi YY, Kim H, Shin SJ, Kim HY, Lee J, Yang HK, et al. Microsatellite instability and programmed cell death-ligand 1 expression in stage II/III gastric cancer: post hoc analysis of the classic randomized controlled study. *Ann Surg.* 2019;270:309–16.
 29. Akagi K, Oki E, Taniguchi H, Nakatani K, Aoki D, Kuwata T, et al. The real-world data on microsatellite instability status in various unresectable or metastatic solid tumors. *Cancer Sci.* 2021;112:1105–13.
 30. Hirabayashi M, Georges D, Clifford GM, de Martel C. Estimating the global burden of Epstein–Barr virus associated gastric cancer: a systematic review and meta-analysis. *Clin Gastroenterol Hepatol.* 2022. <https://doi.org/10.1016/j.cgh.2022.07.042>.
 31. Kanda M, Kasahara Y, Shimizu D, Miwa T, Umeda S, Sawaki K, et al. Amido-bridged nucleic acid-modified antisense oligonucleotides targeting SYT13 to treat peritoneal metastasis of gastric cancer. *Mol Ther Nucleic Acids.* 2020;22:791–802.

Publisher's Note Springer Nature remains neutral with regard to jurisdictional claims in published maps and institutional affiliations.

Springer Nature or its licensor (e.g. a society or other partner) holds exclusive rights to this article under a publishing agreement with the author(s) or other rightsholder(s); author self-archiving of the accepted manuscript version of this article is solely governed by the terms of such publishing agreement and applicable law.